International Journal of Heat and Mass Transfer 52 (2009) 2068–2078

Contents lists available at ScienceDirect

International Journal of Heat and Mass Transfer

journal homepage: www.elsevier.com/locate/ijhmt

Heat conduction with seasonal freezing and thawing in an active layer near a tower foundation

X. Duan [a], G.F. Naterer [b,*]

[a] Department of Mechanical and Manufacturing Engineering, University of Manitoba, 75A Chancellors Circle, Winnipeg, Manitoba, Canada R3T 5V6
[b] Faculty of Engineering and Applied Science, University of Ontario Institute of Technology, 2000 Simcoe Street North, Oshawa, Ontario, Canada L1H 7K4

ARTICLE INFO

Article history:
Received 30 May 2008
Received in revised form 8 November 2008
Available online 16 December 2008

Keywords:
Heat conduction
Permafrost
Power transmission tower
Freezing and thawing
Active layer

ABSTRACT

In this paper, seasonal freezing and thawing of an active layer near a power transmission tower foundation are investigated experimentally with a metal rod buried in an enclosure filled with soil. The measured soil temperatures are used to examine thermal effects of the tower footing and snow cover on seasonal freezing and thawing cycles. It was found that the metal tower has significant thermal effects on the local region around the tower footing. This increases the thaw depth of the active layer and lengthens the freezing/thawing cycle, which adversely affects the foundation stability and safety. These results provide useful new insight of practical utility in the design and maintenance of power transmission line foundations and other infrastructure in northern regions.

1. Introduction

Permafrost, defined as a thermal condition of the ground in which the temperature remains at or below 0 °C for more than 2 years, underlies more than 20% of the land surface of the world and more than 50% of the ground surface of Canada [1,2]. The uppermost layer of the ground over the permafrost table usually experiences seasonal freezing and thawing, due to the seasonal temperature fluctuations. This layer is called an "active layer". Seasonal and long-term thermal changes in the active layer can have significant effects on ecosystem and human infrastructures in northern regions. The frozen ground has good mechanical strength to provide a stable foundation for infrastructure. However, the seasonal freezing/thawing cycle and growth of the active layer thickness (ALT) can lead to severe problems.

During a winter, the formation and resulting expansion of ice in the active layer causes frost heaving [3] and tension forces on a buried structure. In the summer, the thawed active layer loses its mechanical strength and reduces the bond between piles and the ground. It can eventually cause settlement, subsidence and failure of the foundation [4]. Several site monitoring measurements [5–7] and past active layer studies [8–11] have shown an increase of ALT due to climate change. This will likely intensify the problem with infrastructure in northern communities. The U.S. Arctic Research Commission in 2002 organized a series of studies on the impact of global climate change on permafrost in the Arctic and their linkages to natural and human systems [4]. The Geological Survey of Canada initiated research in the Machenzie Valley [12] to examine the impact of permafrost degradation on the surrounding infrastructure. Foundation failure and structural deformation caused by active layer growth and freezing/thawing cycles were found with different types of infrastructure, including old buildings, pipelines, and gas/water distribution systems. Permafrost thawing problems have also been reported for road embankments in northwest China [13].

With increasing concerns about the potentially severe consequences of permafrost degradation, many past studies have developed models and conducted site monitoring studies for the temporal and spatial variations of the active layer. In general, the models can be classified as either numerical, analytical or empirical models. One of the physically-based numerical models is the "simultaneous heat and water" (SHAW) model [14], which has been used mainly in hydrological applications. It estimates the evaporation rate, snow depth, and soil water profiles, in addition to the soil-freezing depth. A similar numerical model was developed by Waelbroeck [8] to estimate the effects of climate change on the thermal regime and moisture of permafrost, as well as the consequences of carbon exchange between the terrestrial biosphere and atmosphere in northern ecosystems. Another similar model was reported by Degaetano et al. [15] to predict seasonal frost penetrations. These models use a daily step in the numerical calculations to predict the detailed ground temperature distribution. This type of modeling strategy accounts for most processes involved in climate–permafrost systems and it can describe gradual changes of seasonal thawing in soils within small temporal inter-

* Corresponding author. Tel.: +1 905 721 8668; fax: +1 905 721 3370.
E-mail address: greg.naterer@uoit.ca (G.F. Naterer).

0017-9310/$ - see front matter © 2008 Elsevier Ltd. All rights reserved.
doi:10.1016/j.ijheatmasstransfer.2008.11.004

Nomenclature

A	amplitude
B	intermediate variable in Eq. (3)
c	specific heat capacity (J/kg·C)
C	volumetric heat capacity (J/m^3 °C)
D	distance, diameter (m, or mm), or intermediate variable in Eq. (3)
h	distance from an element of the heat source to the ground surface (m)
H	height (m, or mm)
k	thermal conductivity (W/mC)
L	length (m or mm)
P	cyclic period (seconds, minutes, or months)
q	heating strength (W/m)
r	radial coordinate (m or mm)
R	radius (m or mm)
T	temperature (°C)
t	time (seconds, minutes, or months)
V	volume (m^3)
w	frequency
z	vertical coordinate (m, or mm)
Z	depth (m, or mm)

Greek

α	thermal diffusivity (m^2/s), or intermediate variable in Eq. (3)
β	intermediate variable in Eq. (3) and Eq. (5)
γ	intermediate variable in Eq. (3)
θ	temperature response or difference (°C)
λ	moisture content (%)
ρ	density (kg/m^3)
σ	intermediate variable in Eq. (3)
ϕ	phase lag

Subscripts

a	active layer
ave	average
b	buried metal rod, or tower
g	ground
gl	ground response to line heat source
gs	ground surface
ps	permafrost
th	thawed soil

vals. However, it requires meteorological data at sparsely spaced locations, which limits its applicability.

An alternative to these approaches is an empirical model based on current climatic statistics and bulk characteristics of the surface and subsurface soil, developed primarily for the practical needs of construction and cold region engineering. The solution of phase change in a homogeneous, semi-infinite medium is a basis for many of these models. It is documented in books by Carslaw and Jaeger [16], Lunardini [1] and Naterer [17]. The quasi-steady approximation to the Neumann problem [10] and Stefan solution [18] is a well-known model used to predict the depth of thaw in soils when little site-specific information is available. The general form and different variations of the Stefan equation have been used frequently for examination of the maximum active layer thaw depth and spatial variability of the active layer [19–21]. Recently, Olguín et al. [22] reported an analytical solution for the coupled heat and mass transfer during the freezing of high water content materials, such as soils and foods. But this approach cannot be used for active layer prediction. Another approximate analytical model is the model developed by Kudryavtsev et al. [23]. It accounts for the effects of snow cover, vegetation, moisture and thermal properties of soil, and regional climate. It provides estimates of the surface temperature and active-layer thickness. It has been widely used for the spatial distribution of the active-layer thickness over a large area [9–11]. Romanovsky and Osterkamp [10] reviewed several analytical solutions for the calculation of active layer thickness. They developed a modified Kudryavtsev equation, which was found to be advantageous over other analytical models (by overcoming the limitation of zero latent heat) and it accurately estimated the active layer thicknesses in the Prudhoe Bay region.

There are also many site observation studies on the permafrost and active layer thickness. An observational network, known as the Circumpolar Active Layer Monitoring (CALM) program, has been implemented to monitor long-term changes in the thickness of the active layer and near-surface temperatures in permafrost regions. This network now includes approximately 125 sites in the Arctic, Antarctic, and several mountainous regions in mid-latitudes [24,25]. Soil temperatures have been monitored continuously at hourly intervals to a depth of 1 m since 1993 in Alaska. An end-of-season thaw depth has been monitored since 1994 at a site near Barrow [5]. A direct correlation was found between the maximum annual thaw depth and the annual thawing degree days at this site. Ref. [10] also reported that the active layer typically reached its maximum thickness and began freezing upward from the bottom, one to two weeks earlier than the beginning of freezing from the surface. Recently, Osterkamp [7] reported data of an experiment initiated in 1977 to determine the effects of climate on permafrost in Alaska. The permafrost temperature and ALT were analyzed together with the variations of climate temperature and snow cover at different sites.

These modeling and site monitoring studies mainly focused on thawing and freezing of the active layer in the vertical direction and its long-term changes with varying climate. But these simplified one-dimensional models cannot take into account the thermal effects of a structure that is built over the permafrost. For many cases these thermal effects, existing in both vertical and lateral directions, can alter the thawing and freezing of the local active layer around a structure [26–29]. Seshadri and Krishnayya [28] developed a quasi-steady method to determine the thaw or frost depth below heated or chilled insulated structures. Krarti et al. [29] used the inter-zone temperature profile estimation (ITPE) procedure to find two-dimensional analytical series solutions for the time-varying heat transfer between the ground and slab-on-grade floors or basements. Previous studies have confirmed that information about thermal effects of a buried structure on the local active layer is important for safety of construction and effectiveness in maintenance of infrastructure in the permafrost regions. This paper will examine these thermal effects of a vertical metal structure in the ground. It extends past studies with power transmission lines [30], which are important elements of infrastructure in northern regions. Built over permafrost regions, the power transmission towers have incurred great capital and labour costs due to maintenance and damage to foundations. Seasonal freezing and thawing of the active layer causes heave, settlement, or tilting, which can break the tower legs, tilt whole towers, buckle tower members, or bend footing members. Thermal effects of the metal tower could

lead to additional thawing around the footing, which intensifies the freezing/thawing cycle. These changes make the foundation problems even worse.

An analytical heat source method has been used widely for transient heat transfer analysis. Solutions of heat conduction problems with various heat sources (point, infinite line, and infinite plane) have been formulated by Carslaw and Jaeger [16]. Multiple point heat sources have been studied in applications to two-dimensional experimental problems [31]. Solutions for single or multiple line sources in a slab and a semi-infinite solid were derived by Saastamoinen [32] using integral transform techniques. The authors developed a variable heating strength model to evaluate the thermal response to a finite line heat source, buried vertically in a semi-infinite medium [33,34]. It was used for a tower foundation problem and it predicted the detailed temporal and spatial distributions of the temperature profiles. No other past studies have been found on the analysis or measurement of the ground thawing problem associated with power transmission towers, so this paper aims to address these shortcomings.

This paper extends previous studies to include the permafrost condition and freezing and thawing processes in the active layer near a power transmission tower foundation. It presents detailed laboratory measurements in a simplified tower foundation under permafrost conditions. A test cell is built to simulate a tower foundation with a single metal rod to represent the tower footing. The permafrost table is simulated by freezing soil in the test cell. Temperature data of typical northern Manitoba sites from Environment Canada are used to design the simulated seasonal temperature variations on the ground surface and around the tower. The thickness of the active layer is determined through temperature measurements and compared with results calculated by the modified Kudryavtsev equation [10]. Thermal effects of the metal tower are analyzed by examining the changes caused on the ground temperature fluctuations, and the thawing depth of the active layer around the tower footing. The effects of snow cover are examined by providing a different simulated temperature (under snow cover) to the soil surface in the test cell. Ground temperature characteristics and active layer thickness with snow on the surface are compared to those without snow. These new data will provide valuable insight for the design and maintenance of foundations of power transmission line towers and other structures in permafrost regions.

2. Approximate analytical model of ground heat transfer

In this section, a modified Kudryavtsev equation [10] is extended to the calculation of the active layer thawing depth in a simulated tower foundation (see problem schematic in Fig. 1). The temperature of the ground surface is assumed to have the following form of harmonic oscillation

$$T_{gs}(t) = T_s + A_{gs}\sin\left(\frac{2\pi t}{P}\right) \tag{1}$$

where T_s is the mean annual temperature at the ground surface, °C; A_{gs} is the amplitude of annual temperature variations at the ground surface, °C; P is the period of temperature variation (one year), s. The active layer thaw depth, Z_a, is expressed by the following equation [10,11]:

$$Z_a(2\bar{A}C_{th}+Q_{ph}) = 2(A_{gs}-|\bar{T}_{ps}|)\sqrt{\frac{k_{th}C_{th}P}{\pi}} + \frac{(2\bar{A}C_{th}Z_{2c}+Q_{ph}Z_a)Q_{ph}\sqrt{\frac{k_{th}P}{\pi C_{th}}}}{2\bar{A}C_{th}Z_{2c}+Q_{ph}Z_a+(2\bar{A}C_{th}+Q_{ph})\sqrt{\frac{k_{th}P}{\pi C_{th}}}} \tag{2}$$

where

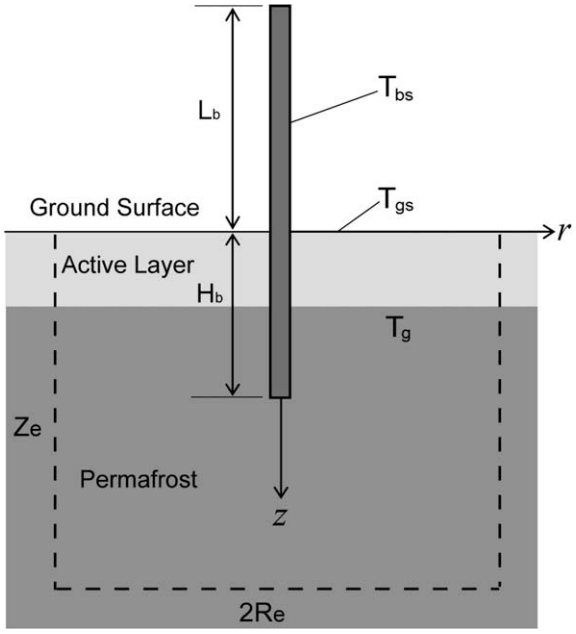

Fig. 1. Schematic of a simplified tower foundation – a metal rod buried in permafrost.

$$\bar{A} = \frac{A_{gs}-|\bar{T}_{ps}|}{\ln\frac{A_{gs}+\frac{Q_{ph}}{2C_{th}}}{|\bar{T}_{ps}|+\frac{Q_{ph}}{2C_{th}}}} - \frac{Q_{ph}}{2C_{th}} \quad \text{and} \quad Z_{2c} = \frac{2(A_{gs}-|\bar{T}_{ps}|)\sqrt{\frac{k_{th}C_{th}P}{\pi}}}{2\bar{A}C_{th}+Q_{ph}}$$

and $\bar{T}_{ps}$ is the mean annual permafrost surface temperature, °C; C_{th} is the volumetric heat capacity of thawed soil, J/m^3 °C; k_{th} is the thermal conductivity of the thawed soil, W/m °C; and Q_{ph} is the volumetric latent heat of phase change (of water in the soil), J/m^3.

The equation can be simplified by introducing the following dimensionless variables, $\alpha = \frac{2C_{th}A_{gs}}{Q_{ph}}$ and $\beta = \frac{2C_{th}\bar{T}_{ps}}{Q_{ph}}$, which are analogous to the Stefan number (the ratio of sensible and latent heats) in the Neumann equation. Using these two new variables, the active layer thawing depth can then be expressed as follows:

$$Z_a = Z^*\sqrt{\frac{k_{th}P}{\pi C_{th}}} \tag{3.1}$$

where Z^* is a solution to the following quadratic equation

$$Z^*\frac{\alpha-\beta}{\ln\frac{\alpha+1}{\beta+1}} = \alpha-\beta+\frac{Z^*+\alpha-\beta-\ln\frac{\alpha+1}{\beta+1}}{Z^*+\alpha-\beta-\ln\frac{\alpha+1}{\beta+1}+\frac{\alpha-\beta}{\ln\frac{\alpha+1}{\beta+1}}} \tag{3.2}$$

The solution of the above quadratic equation can be expressed as

$$Z^* = B+\sqrt{B^2+D} \tag{3.3}$$

where

$$B = \sigma+\frac{\sigma}{2\gamma}-\frac{\gamma}{2\sigma}-\frac{\gamma}{2}, D = \sigma+\sigma\gamma+\gamma-\sigma^2-\frac{\sigma^2}{\gamma}, \quad \text{and} \quad \gamma = \alpha+\beta, \quad \sigma = \ln\frac{\alpha+1}{\beta+1}$$

The ground temperature response to a seasonally varying heat source can be predicted by a variable heating strength model [33,34]. The model provides a good approximation of the seasonal thermal effects of the tower on the temperature variations near the tower foundation. The thermal response at a ground point, $P(r,z)$, to the finite line heat source, $q(h,t)$, can be obtained by a method of images and integration of a series of time-varying point heat sources as follows:

$$\theta_{gl}(r,z,t)=\frac{1}{8\pi^{1.5}k_g\sqrt{\alpha_g}}\int_0^H\int_0^t\frac{q(h,t')}{(t-t')^{1.5}}\times\left\{\exp\left[-\frac{D_1^2}{4\alpha_g(t-t')}\right]-\exp\left[-\frac{D_2^2}{4\alpha_g(t-t')}\right]\right\}dt'dh \quad (4)$$

where $D_1=\sqrt{r^2+(z-h)^2}$, $D_2=\sqrt{r^2+(z+h)^2}$, h is the distance from an element of the heat source to the ground surface, m; θ_{gl} is the thermal response, °C; k_g is the thermal conductivity of the ground, W/m °C; and α_g is the thermal diffusivity of the ground, m^2/s.

The solution of Eq. (4) can be expressed alternatively with respect to the following variables: $\beta_1=\frac{D_1(t-t')^{-0.5}}{2\sqrt{\alpha_g}}$, $\beta_2=\frac{D_2(t-t')^{-0.5}}{2\sqrt{\alpha_g}}$:

$$\theta_{gl}(r,z,t)=\frac{1}{2\pi^{1.5}k_g}\int_0^H\left[\frac{1}{D_1}\int_{\frac{D_1}{2\sqrt{\alpha_g t}}}^{\infty}q\left(h,t-\frac{D_1^2}{4\alpha_g\beta_1^2}\right)e^{-\beta_1^2}d\beta_1-\frac{1}{D_2}\int_{\frac{D_2}{2\sqrt{\alpha_g t}}}^{\infty}q\left(h,t-\frac{D_2^2}{4\alpha_g\beta_2^2}\right)e^{-\beta_2^2}d\beta_2\right]dh \quad (5)$$

The seasonal variation of the line heat source was approximated by the following sinusoidal expression

$$q(h,t)=q_m+A_q\sin(w_2t+\phi_2) \quad (6)$$

where q_m is the average value of the heat source, A_q is the amplitude of the seasonal variation, w_2 is the frequency of variation, and ϕ_2 is the phase lag.

Using a variable heating strength model, the thermal response to this line heat source can be evaluated by either Eqs. (4) or (5). In particular, the long-term thermal response can be calculated by the following approximate solution to this sinusoidal line heat source, which needs much less computational time,

$$\theta_{gl}(r,z,t)=\frac{q_m}{4k_g\pi}\int_0^H\left[\frac{1}{D_1}erfc\left(\frac{D_1}{2\sqrt{\alpha_g t}}\right)-\frac{1}{D_2}erfc\left(\frac{D_2}{2\sqrt{\alpha_g t}}\right)\right]dh+\frac{A_q}{4\pi k_g}\int_0^H\left\{\left[\frac{e^{-D_1\sqrt{\frac{w_2}{2\alpha_g}}}}{D_1}\sin\left(w_2t-D_1\sqrt{\frac{w_2}{2\alpha_g}}+\phi_2\right)\right]-\left[\frac{e^{-D_2\sqrt{\frac{w_2}{2\alpha_g}}}}{D_2}\sin\left(w_2t-D_2\sqrt{\frac{w_2}{2\alpha_g}}+\phi_2\right)\right]\right\}dh \quad (7)$$

In the next section, results of an experimental study on the active layer near a tower foundation will be presented. The measured active layer thickness will be compared with calculated values from the simplified Kudryavtsev model. More importantly, seasonal thermal effects of the metal tower and local alteration of the ALT caused by these thermal effects will be studied. The experimental results can be integrated with the simplified Kudryavtsev model for estimation of the local ALT near a buried structure in the permafrost regions.

3. Experimental design and apparatus

Under typical permafrost conditions, the amplitude of the annual ground temperature oscillation decreases at lower levels in the ground. The point where there is no discernable change in ground temperature is called the "depth of zero annual amplitude". Below this depth, ground temperature changes are very small throughout the year. When a power transmission line tower is buried under the ground, the annual ground temperature variations will be altered by the thermal effects of the tower footing.

This section simulates a simplified tower foundation (depicted in Fig. 1), where a vertical metal rod is used to represent the tower footing. The simplified tower has an above-ground part, L_b, and an underground part, H_b. The surface temperature of the tower is T_{bs} and the ground surface temperature is T_{gs}. In this problem, the domain is approximately a semi-infinite half-space in the lateral (r coordinate) and vertical (z coordinate) directions. An equivalent "effective area" (or examined area) of heat transfer will be examined. It is expressed as $R_e \times Z_e$ in a two-dimensional system (depicted in Fig. 1). This area has been carefully calculated, so that it surpasses the local space to which thermal effects of the tower footing are confined. Also, the depth must lie beyond the depth of zero annual amplitude. The dimensions of this examined area were calculated to be Z_e = 12 m and R_e = 6 m for the weather conditions of a northern Manitoba tower foundation [34].

The dimensions of the experimental test cell were obtained by scaling down the dimensions of the examined area and simplified tower footing (metal rod with a diameter of 0.4 m and a buried depth of 4 m). The scaling factor was determined from a dimensional analysis of heat conduction in the ground, which yielded a temperature scale of 1:1, length scale of 1:60, and time scale of 1:3, 600. Using this method, the experimental test cell was designed with the following dimensions: examined area of 200 mm in depth, 200 mm in diameter centered on a metal rod of D_b = 6.67 mm diameter, and H_b = 66.67 mm buried in the ground. The annual cycle of temperature variations in the foundation for 365 days was then simulated in the test cell over a time of P = 146 min. The test cell was constructed as a cubical enclosure with four side walls tangential to the outer surface of the scaled examined area. Fig. 2 shows the detailed experimental setup. The container is made with 2.54 cm thick Plexiglas and an inner volume of 200 mm × 200 mm × 200 mm filled with soil to simulate the examined area of the simplified tower foundation. An additional layer of composite fabric was used for further insulation purposes.

The soil used in this study was obtained from a field site near a tower foundation in Oshawa, Ontario. It is a well-graded silty sand (loam) that contains 46.2% silt, 48.5% sand, and traces of gravel (2.6%) and clay (2.7%). The porosity of this type of soil ranges from 23% to 47% at the field site and it was 38% in the experiments. Additional moisture was added into the soil sample to make it similar to soil in permafrost regions. The soil was mixed thoroughly to reach a uniform structure before its properties were measured. In the upcoming experimental studies, soil in the test cell was measured to have a bulk density of ρ_{soil} = 1174 kg/m^3 and moisture of λ_{soil} = 16.5%. Detailed information about these measurements and other thermal properties of the soil, particularly the thermal conductivity and thermal diffusivity, will be discussed in Section 4.1.

A multi-pass plate heat exchanger, with temperature controlled fluid circulating within it, was installed on the top of the enclosure to provide the desired ground surface conditions. The bottom plate of the heat exchanger was made from Aluminum, while the cover was made of stainless steel. The inner surfaces of this heat exchanger were coated with a thin layer of Epoxy for protection against corrosion. The plate heat exchanger was enclosed by the walls of the container and the Plexiglas cover of 20 mm thickness. A circular heat exchanger was designed together with an aluminum rod to represent the tower footing. It can be inserted into the container through a hole located at the center of the cover. A temperature controlled fluid then circulates around the finned part of the rod inside the circular heat exchanger, to simulate the annual variations of the air temperature around the above-ground portion of a tower. The shell of this heat exchanger was made with ABS for insulation purposes. The 3 mm thick ABS shell was wrapped with

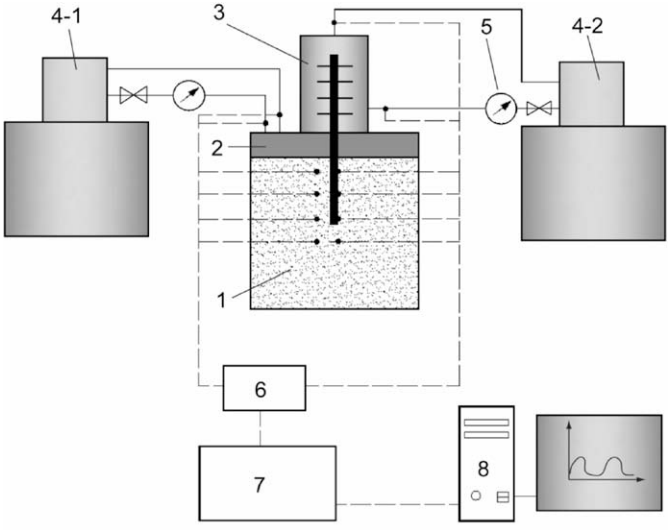

1: soil container, 2: plate heat exchanger, 3: circular heat exchanger and aluminum rod, 4 Neslab temperature controlled baths ULT-80 (4-1) and RTE 140 (4-2), 5: FTB603B flow sensors 6: thermocouple analog input module NI9211, 7: USB chassis for cDAQ-9172, 8: Computer and data logger program, • : thermocouples

Fig. 2. Schematic of the experimental system.

another layer of composite fabric of 8 mm thickness to provide additional thermal insulation.

The circulating fluids for both the plate and circular heat exchangers were supplied by two NESLAB heating and refrigerating baths, ULT-80 and RTE 140, respectively. The ULT-80 bath can provide a temperature range of −80 °C to +10 °C, with a stability of ±0.03 °C. The RTE 140 can provide a temperature range of −40 °C to +150 °C, with a stability of ±0.05 °C. Since the temperature range in this study varies from −30 °C to +10 °C, a non-freezing fluid is used, which is a 50/50 mixture, by volume, of filtered tap water and ethylene glycol. The flow rates of the circulating water were measured with Omega FTB603B flow sensors. To realize continuous temperature variations of the baths, a remote control scheme was developed. A NESCOM program was used to display and control the bath temperatures. With a USB-to-Serial Converter, controlling signals from the computer were sent to the controllers of the baths.

A computer data acquisition system was used for the temperature measurements, including 15 T-type thermocouple (TC) probes (Omega) that were inserted horizontally into the enclosure at different locations through three sides of the Plexiglas walls, with 5 TCs on each side. The radial distance, R, between the TCs and the aluminum rod was the same for each side, but it varied for different sides, as shown in Table 1. Another 8 T-type thermocouples were installed at the inlets and outlets of the two heat exchangers to monitor the circulating fluid temperatures. The thermocouples were connected to six Thermocouple Analog Input (TAI) Modules NI 9211 (National Instruments) with a differential connection mode. Each TAI module provided 4 channel inputs. The TAI modules were connected to a cDAQ-9172 (National Instrument) chassis, which is connected to the computer for data acquisition through the NI-DAQmx software.

Efforts were made to minimize experimental errors and uncertainties as much as possible. T-type thermocouple wires were used to connect the inserted thermocouple probes and the input modules. These wires were made as short as possible to reduce the uncertainty in the measured temperature, which was the most important parameter in this study. An uncertainty analysis was conducted by the method of Kline and McClintock [35]. The results are summarized in Table 2. The uncertainty of the measured temperature includes the cold-junction compensation sensor accuracy, errors caused by the NI9211 modules, as well as the accuracy of the thermocouple measurement probe itself. Time was recorded in the VI logger based on the CPU time for transient temperature measurements. The precision limit was assumed negligible. The bias limit arose from the inaccuracy of defining the starting time of the measurements, which lies in the range of 5 s.

Table 1
Thermocouple (TC) positions.

Side 1, R = 39 mm		Side 2, R = 14 mm		Side 3, R = 7 mm	
TC #	z (mm)	TC #	z (mm)	TC #	z (mm)
0	9.5	5	8.5	10	13.5
1	23.5	6	21	11	23.5
2	41	7	38.5	12	38.5
3	58	8	58.5	13	56
4	74.5	9	76	14	73.5

Table 2
Summary of measurement uncertainties.

Parameter	Uncertainty
Temperature, T	±1.3 °C
TC positions: radial distance, R	±1.2 mm
Vertical distance, z	
Diameter of the metal rod, R_b	±0.5 mm
Buried length of the metal rod, H_b	±1.1 mm
Density of soil, ρ_{soil}	±2.37%
Thermal conductivity of soil, k_{soil}	±5%
Thermal diffusivity of soil, α_{soil}	±20%
Moisture content of soil, λ_{soil}	0.003 m^3/m^3

4. Results and discussion

4.1. Soil thermal properties

Thermal properties of soils vary significantly for different soil types, moisture contents, and packing of soil [36,37]. As a result, measurements were performed for the specific properties of soil in this study. These properties include the bulk density, ρ_{soil}, moisture content, λ_{soil}, thermal conductivity, k_{soil}, and thermal diffusivity, α_{soil}. The volume of the soil container was calculated to be $V_{cell} = 7.45 \times 10^{-3}\ m^3$. The total mass of the soil in the enclosure, m_{soil}, was measured with a Starfrit electric scale, after which the density of soil was calculated by $\rho_{soil} = m_{soil}/V_{cell}$. The moisture (volumetric water content, VWC) of the soil was measured by an EC-5 ECH2O soil moisture sensor (Decagon Devices, Inc.). A Hukseflux TP01 soil property sensor was used to measure the thermal conductivity and diffusivity of the soil. The TP01 sensor determines the thermal properties of a medium from its temperature response to a heating pulse. A power supply of about 1.5 VDC was provided to the TP01 sensor. The NI data acquisition system measured the transient voltage response signals, which were then processed to determine the thermal properties.

Thermal conductivity and diffusivity depend on the soil moisture and temperature. Fig. 3 shows the measured thermal properties of soil samples from the test cell, with different moisture contents and temperatures. It can be observed from Fig. 3a that the frozen soil has a higher thermal conductivity than the unfrozen soil. This occurs because of the higher thermal conductivity of ice (2.03 W/m °C at −20 °C) compared to that of liquid water (0.56 W/m °C at 0.01 °C). When the liquid water in the soil pores becomes ice, the apparent thermal conductivity of the soil increases. But the thawed soil retains a relatively constant thermal conductivity. Also, the frozen soil has a much higher thermal diffusivity than the thawed soil. Similarly, this arises because the thermal diffusivity of ice (approximately $11.6 \times 10^{-7}\ m^2/s$) is much higher than that of liquid water (approximately $1.42 \times 10^{-7}\ m^2/s$). Fig. 3b shows that the thermal conductivity increases dramatically for higher water content, when water replaces the air voids in the soil. The thermal diffusivity shows a more complex variation trend. At very low moisture levels, the thermal diffusivity of the soil increases with higher moisture content, due to the increase of bulk thermal conductivity with more water that displaces air in the soil void. The thermal diffusivity reaches a maximum of $4.5 \times 10^{-7}\ m^2/s$ with approximately a moisture content of 23%. Then it decreases with more moisture. This can be explained by the more significant increase of bulk soil heat capacity with more water content. Water has a greater heat capacity ($4.19 \times 10^6\ J/m^3\ K$) than dry silt ($1.13 \times 10^6\ J/m^3\ K$) and sand (approximately half the value for silt) [5].

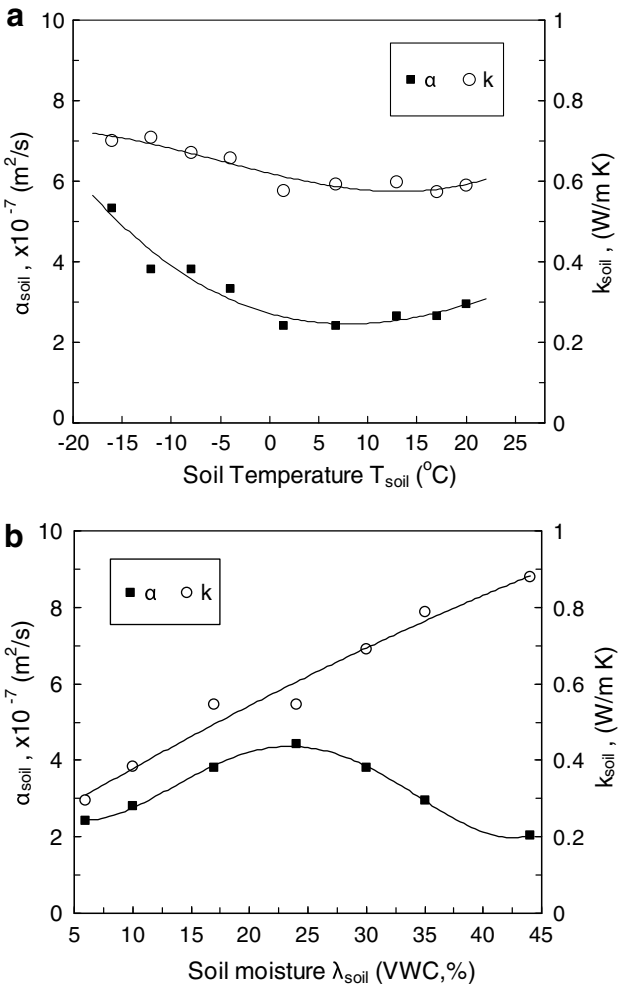

Fig. 3. Soil thermal conductivity and diffusivity at different temperatures and moisture contents: (a) λ_{soil} = 16.5%, (b) Soil temperature = 20 °C.

4.2. Seasonal freezing and thawing without a tower

The seasonal thermal process in the active layer is complex. Heat conduction usually dominates in the cold winters. But in other seasons, the thermal processes may involve heat conduction, moisture migration, vapour transportation, and ice segregation. This study is not intended to examine all detailed effects in the ground, as they have been studied previously (references cited in Section 1). Instead, this experimental study will simulate a simplified tower foundation in permafrost conditions and measure the seasonal temperature variations within the foundation under different ground surface and tower surface temperatures.

In order to simulate a permafrost table in the test cell, the ULT-80 refrigerated bath was used to circulate fluids at −20 °C through the plate heat exchanger, at the top surface of the soil enclosure. The soil temperature started to drop and then the soil froze downward. After 20 h of circulation, the soil in the test cell reached a nearly steady state, with sub-zero temperatures at all measurement points. The nearly linear temperature distribution in the vertical direction is shown in Fig. 4. The dashed line shows a linear

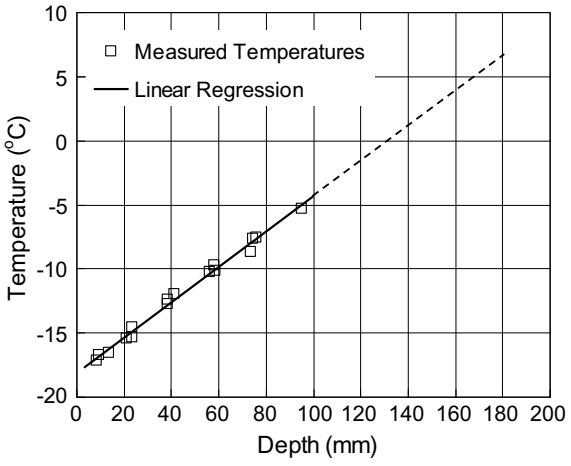

Fig. 4. Simulated permafrost temperatures.

extrapolation of the soil temperature beyond the measured depth. Fig. 4 shows that a permafrost table was created down to a depth of about 135 mm.

After the permafrost table was created, the simulated seasonal ground surface temperature was then applied (starting with −20 °C) to examine the temperature variations in the foundation, without a tower. This was realized by circulating fluids with periodic temperature variations (from the ULT-80 bath) through the top plate heat exchanger. In order to have realistic periodic temperature variations to represent the seasonal temperature variations in northern Canada, the Canadian Climate Normals or Averages data (1971–2000) recorded by Environment Canada [38] was used. Fig. 5 shows the daily averaged air temperatures from three sites in northern Canada: Thompson Airport (Manitoba), Churchill Airport (Manitoba), and Sachs Harbour Airport (Northwest Territories). The designed temperature is 5 °C lower in each month than the corresponding temperatures at the Thompson Airport. It can be approximated as follows:

$$T_{\text{air}}(t) = -8.5 + 19\cos\left(\frac{2\pi t}{146} - 1.18\pi\right) \tag{8}$$

When there is no snow cover, $T_{gs}(t) = T_{\text{air}}(t)$ was assumed.

Fig. 6 shows the measured results of the ground temperatures at 5 representative positions in the foundation for a period of 292 min (corresponding to two years in a real ground situation). At most positions, the ground temperatures remain frozen, indicating the permafrost table. At positions located in the active layer (z = 8.5 mm in Fig. 6), the soil temperature undergoes thawing in the "summer" and freezing in the other period. Fig. 7 illustrates the highest "summer" ground temperatures in the foundation. It clearly shows that the ground temperature decreases dramatically with depth in the top soil levels. The results also confirm the one-dimensionality of these measurements, since temperature readings from thermocouples of three sides fall onto the same trend line. The active layer thaw depth can be found by examining the depth level where the ground temperatures reach 0 °C, at around 13 mm in this measured case. Using the ground surface temperature parameters in Eq. (8), together with the soil and water thermal properties in Eq. (3) with $\bar{T}_{ps}$ = 0, yields an active layer thawing depth of 13.6 mm, which agrees well with the measured data.

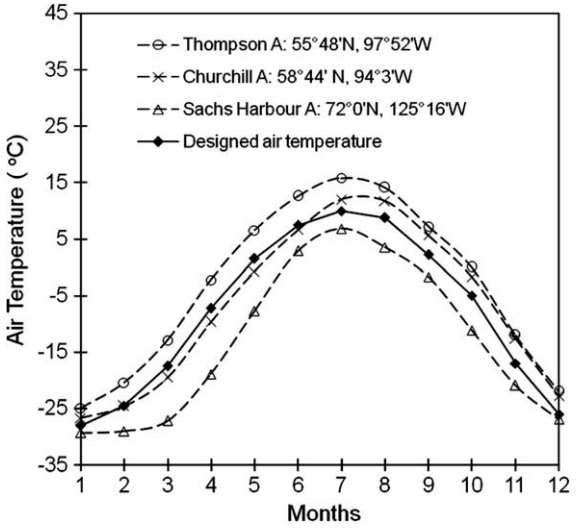

Fig. 5. Air temperature at different permafrost locations and simulated air temperature.

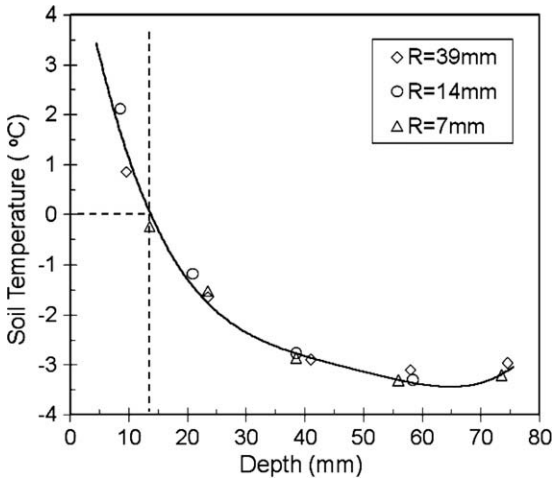

Fig. 7. Summer ground temperatures without a tower (active layer thawing depth shown by the vertical dashed line).

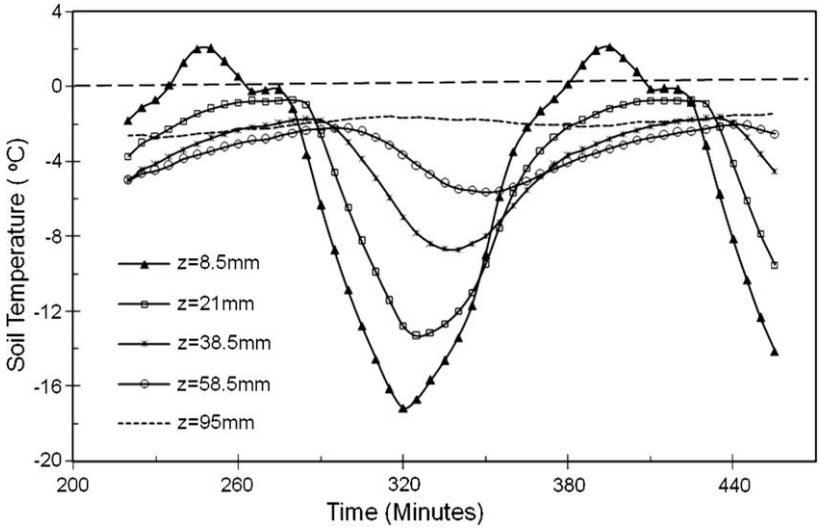

Fig. 6. Foundation ground temperature variations without the tower.

4.3. Thermal effects of the tower on the local active layer

The main purpose of this study is to find thermal effects of the metal tower on the seasonal freezing and thawing around the foundation. After the seasonal simulation was performed over 530 min, the circular heat exchanger was installed onto the test cell, with the aluminum rod inserted into the soil to represent a metal tower footing. This time corresponds to an early summer season for easy installation of the tower. Fluids from the RTE 140 bath then circulated through the circular heat exchanger to simulate air flow around the tower. The bath temperature was controlled by the same design temperature expressed in Eq. (8), as $T_{gs}(t) = T_{air}(t)$ without snow cover. Then the freezing and thawing processes can be examined from the temperatures measured at different locations in the tower foundation.

To characterize thermal effects of the tower, several statistical parameters of the measured ground temperatures in two cycles (292 min) were analyzed and compared to measured temperatures without the tower in the corresponding period. These parameters include: (1) the average temperature, T_{ave}; (2) the highest temperature, T_{max}; (3) the lowest temperature T_{min}, and (4) the amplitude of the temperature oscillation, A_T. Fig. 8 shows the average and amplitude of the ground temperatures at different locations. Parameters with an asterisk (*) refer to temperatures with the tower and those without asterisks are temperatures without the tower. In Fig. 8a, the temperature average T_{ave} shows a slight increase at most locations, with less increase for points closer to the tower footing. Fig. 8b shows the relative increase of the temperature amplitude, $(A_T^* - A_T)/A_T$, around the tower footing, indicating its thermal effect on ground temperatures. It can be observed that this thermal effect varies in both radial and vertical directions. In the radial direction, it decreases with further distance from the tower footing (with almost no change at $R = 39$ mm). In the vertical direction, the effect is most significant around the middle and lower portion of the tower footing, but insignificant at the top and deeper levels below the buried depth of the tower.

Fig. 9 shows the measured soil temperatures in the foundation at two typical times, $t = 688$ min and $t = 625$ min, which approximately correspond to a particular time in the "summer" and another time in the "winter". As compared to the summer temperatures in Fig. 7, the ground temperatures with the tower reveal a two-dimensional character. Since thermocouples with $R = 39$ mm are relatively far away from the metal rod, the temperatures at these positions are almost the same as those without the tower. In the "summer" (Fig. 9a), the tower footing makes the surrounding soil warmer. This effect increases at locations closer to the tower footing (as expected). This thermal effect causes additional thawing and makes the active layer increase in a local region around the tower footing. This can be readily observed with the two-dimensional temperature contours shown in Fig. 10, which were created in Matlab by interpolations of the measured temperatures. The isotherm of 0 °C approximately indicates the level of active layer thawing, which is around 13 mm at locations far from the tower footing, but increases to a level of about 19 mm at locations very close to the footing. Similarly at $t = 625$ min ("winter"), the tower footing makes the surrounding soil colder and causes an additional freezing effect. As discussed in the introduction section, this intensified thawing and freezing could result in more severe heave and settlement of the tower and structural damage to the transmission lines.

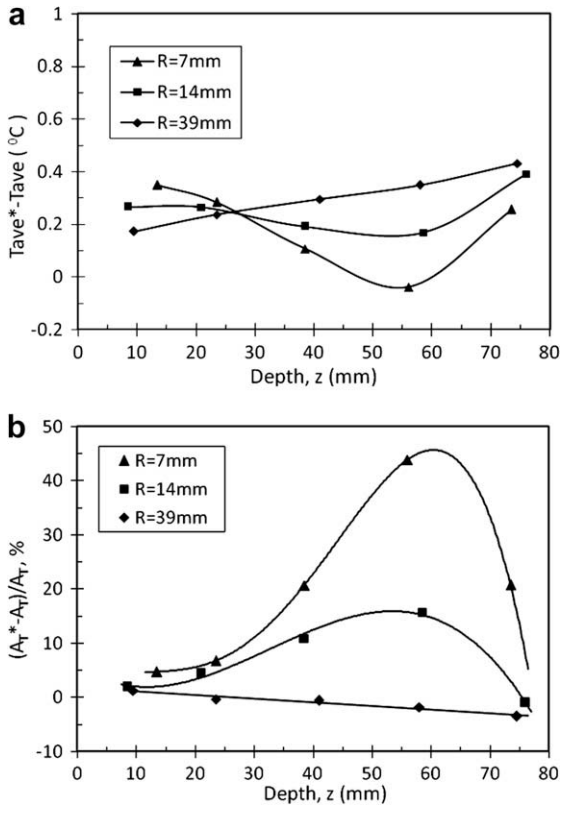

Fig. 8. Difference of (a) average and (b) amplitude of ground temperature variations with and without the tower (* denotes temperatures with the tower).

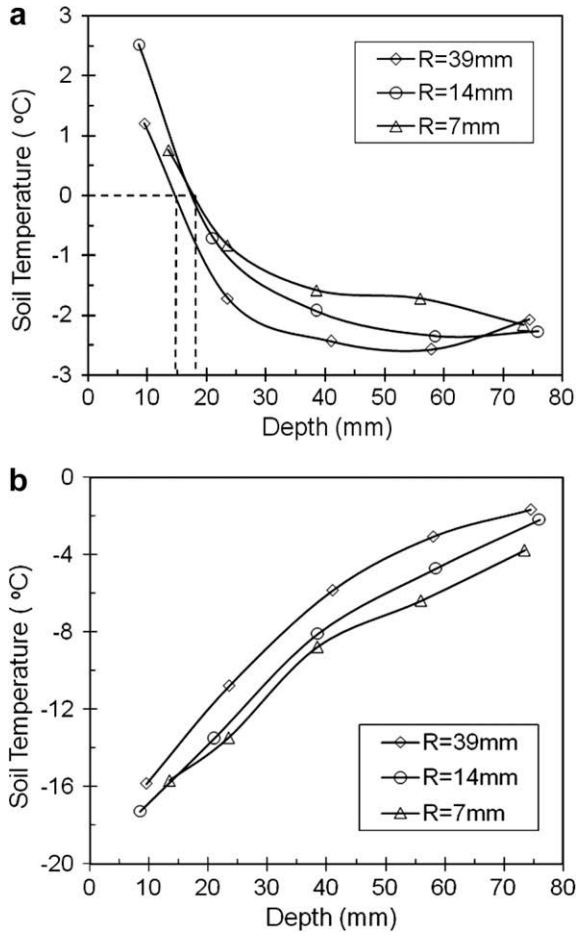

Fig. 9. Thermal effects of the tower footing on (a) thawing in the foundation in the summer, $t = 688$ min, and (b) freezing in the foundation in the winter, $t = 625$ min.

Further analysis of the results in Fig. 9 reveals that thermal effects of the tower footing are not uniform within the foundation. It varies not only with time, but also at different positions around the tower footing. In the vertical direction, these thermal effects start from zero at the ground surface and increase to a maximum level at a certain depth (about 60 mm in the current example). Then it decreases to zero at another depth beyond the buried depth of the tower footing. This variation agrees with the changes of temperature amplitude shown in Fig. 8b. It can be concluded that thermal effects are confined to a limited local space surrounding the tower footing.

The seasonal thermal effects of the tower are caused by seasonal variations of air temperature and the large difference between thermal properties of the metal tower and the foundation. The buried metal structure has a much higher thermal conductivity and diffusivity than the soil. In the summer, the air temperature is usually higher than the ground temperature and heat is conducted through the tower downwards into the ground. This leads to an additional temperature increase of the surrounding soil. In the winter, the air temperature is usually colder than the ground temperature, thereby causing heat flow from the ground to the surrounding air.

4.4. Effects of snow cover

Snowfall and the duration of snow cover influence the permafrost distribution and thickness by controlling heat transfer to the ground from the atmosphere. Heavy snowfall insulates the ground from severe winter cold. This warming effect prevents permafrost aggradation. Thick snow cover in the spring has a cooling effect. It delays the spring thaw and it can promote permafrost aggradation [3]. On the other hand, infiltrating snow meltwater in the spring increases the soil moisture. It can cause rapid warming of the upper soil layer, due to the higher heat capacity of water compared to frozen soil [5]. In this study, the snow melt and water infiltrating processes will not be considered in the experiments. Instead, a simplified method will be used, by providing a ground surface temperature under the cooling and warming effects of snow cover. In the experimental setup, the same air temperature expressed by Eq. (8) was provided to the circular heat exchanger (representing the tower), but a new ground surface temperature under the effects of snow cover was provided to the soil surface through the plate heat exchanger. This ground surface temperature was designed according to the 5 cm depth soil temperatures at the Thompson Airport (Manitoba) recorded by the Environment Canada [36], with the same 5 °C difference used for the air temperature simulation. The simulated ground surface temperature is shown in Fig. 11, as compared with the simulated air temperature. This new soil surface temperature has similar values to the air temperature in the summer. In other seasons, however, it is substantially different than the air temperature, due to the thermal effects of the snow. It can be approximated by the following function

$$T_{gs}(t) = -1 + 11\cos\left(\frac{2\pi t}{146} - 1.2\pi\right) \tag{9}$$

With this new surface temperature, the foundation temperatures also change, as shown in Fig. 12. With snow cover in the winter, ground temperatures are higher than those without snow (as expected). It can be observed that this difference is more significant at shallow depths. Fig. 13 shows the changes of the average and amplitude of ground temperature oscillations at different locations. Parameters with two asterisks (**) denote temperatures with snow. The average temperature T_{ave} increases, as indicated by positive values of $T^{**}_{ave} - T^{*}_{ave}$ for all measured points in Fig. 13a. Also, the difference of $T^{**}_{ave} - T^{*}_{ave}$ (caused by snow cover) decreases with depth. On the other hand, Fig. 13b shows negative values of $A^{**}_{T} - A^{*}_{T}$ for all measured points, indicating a decrease of the temperature amplitude. Again, this effect varies in the radial direction, due to thermal effects of the tower footing.

Fig. 14 shows ground temperatures in the foundation in summer and winter times corresponding to the typical times of Fig. 9. As a response to the thermal effects of snow cover, the winter temperatures increase significantly and the summer temperature also shows a slight increase. Thermal effects of the tower (illustrated by temperature differences at different radial distances from the tower footing) show the same distribution as Fig. 9. Under these conditions, the thawing depth of the active layer also increased to 15 mm at locations far from the tower footing and 24 mm immediately around it, as shown in Fig. 15. These results confirm that snow cover leads to higher ground temperatures and increased active layer thawing depths, which have adverse effects on foundation protection in permafrost regions.

5. Conclusions

This paper has presented new results from experimental studies of ground freezing and thawing in a simplified power transmission tower foundation. Seasonal ground temperatures were measured in an experimental test cell under different operating conditions.

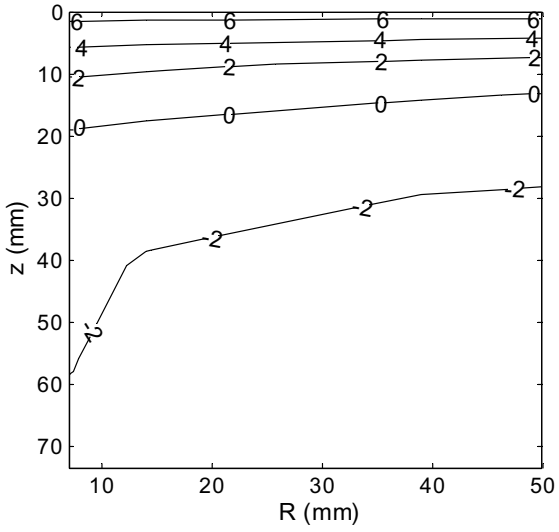

Fig. 10. Two-dimensional contour of ground temperatures in the summer. The temperature gradient and active layer thawing depth in the lateral direction indicate thermal effects of the tower footing.

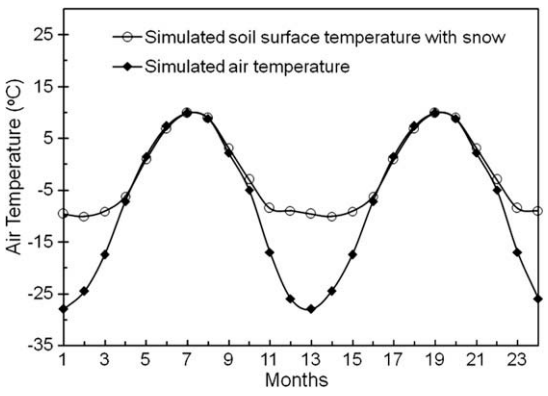

Fig. 11. Simulated air and soil surface temperatures with snow cover.

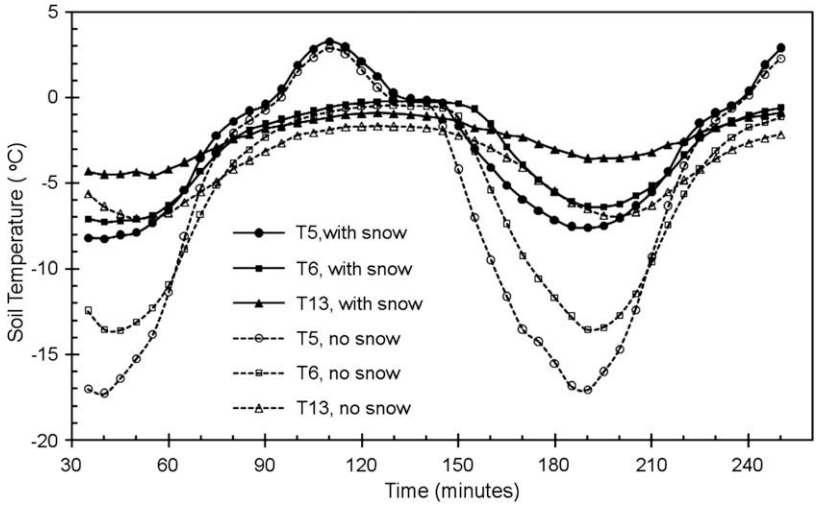

Fig. 12. Comparison of seasonal active layer temperature variations at three locations around the tower footing, with and without snow cover (measurement points: T5: $R = 14$ mm, $z = 8.5$ mm; T6: $R = 14$ mm, $z = 21$ mm; T13: $R = 7$ mm, $z = 56$ mm).

These temperatures were analyzed to determine thermal effects of the buried tower footing and effects of the modified ground surface temperature with winter snow cover, especially the effects on the active layer thaw depth. This study has found that a buried metal structure changes the temperature profiles of the foundation, particularly in a certain "effective space" around the tower footing. The measured active layer thaw depths agree well with calculated values using the modified Kudryatsev equation, when there is no tower, or locations far from the tower footing (outside the effective space). Thermal effects of the tower introduce additional tempera-

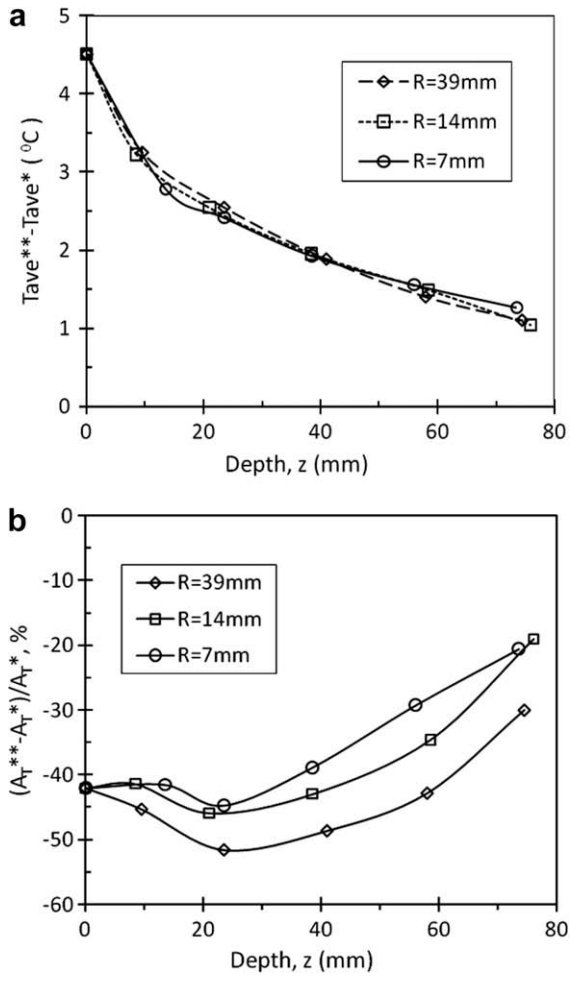

Fig. 13. Effects of snow on the average, Tave, and amplitude, AT, of ground temperatures (* denotes temperatures with the tower, ** denotes temperatures with snow cover).

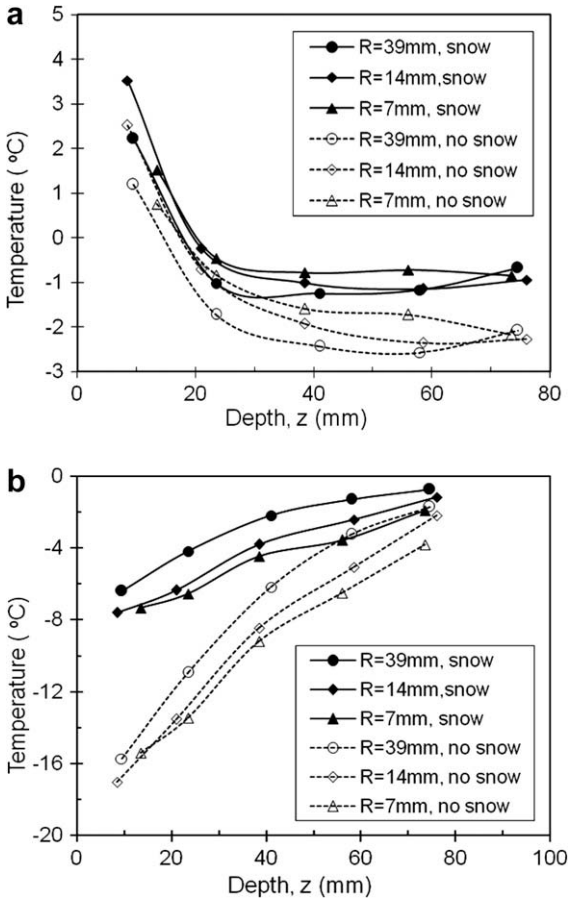

Fig. 14. Comparison of (a) summer and (b) winter ground temperatures at different locations around the tower footing with and without snow on the ground surface.

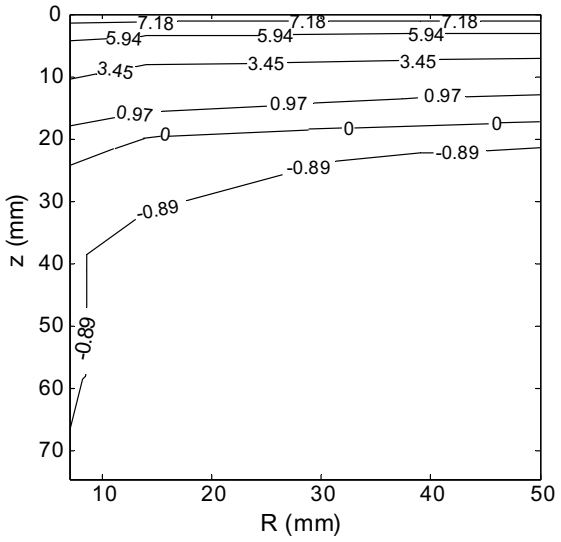

Fig. 15. Contour of ground temperatures in the summer, with snow cover in the winter.

ture increases in the "summer" and therefore lead to increased active layer thaw depths around the tower footing. It also causes additional temperature decreases and freezing in the "winter". The enhanced thawing and freezing cycle could make the permafrost problem even worse for foundations of power transmission lines and other similar buried metal structures. This factor must be taken into account in maintenance of existing structures and design of new towers. This study also showed that the snow cover leads to higher ground temperatures and increased active layer thawing, which affect the foundation protection in permafrost regions. Based on the comparison of ground temperatures with and without snow cover, a technique of removing or preventing the winter snow over a tower foundation could help to keep the ground frozen and increase the foundation safety. Results from this experimental study provide valuable new insight for the design and maintenance of foundations of power transmission line towers and other structures in permafrost regions.

Acknowledgments

Support of this research from Manitoba Hydro (particularly Dr. M. Lu and Mr. W. Mueller), Natural Sciences and Research Council of Canada (NSERC), and a University of Manitoba Graduate Fellowship (X. Duan), is gratefully acknowledged.

References

[1] V.J. Lunardini, Heat Transfer in Cold Climates, Van Nostrand Reinhold Co., NY, 1981.
[2] Natural Resource of Canada, <http://gsc.nrcan.gc.ca/permafrost/wheredoes_e.php>.
[3] Alaska Regional Profiles, Northwest Region, <http://www.alaskool.org/resources/regional/nw_reg_pro/permafrost.html>.
[4] U.S. Arctic Research Commission Permafrost Task Force Climate Change, Permafrost, and Impacts on Civil Infrastructure, Special Report 01-03, U.S. Arctic Research Commission, Arlington, Virginia, 2003.
[5] K.M. Hinkel, F. Paetzold, F.E. Nelson, J.G. Bockheim, Patterns of soil temperature and moisture in the active layer and upper permafrost at Barrow, Alaska: 1993–1999, Global Planet. Change 29 (3) (2001) 293–309.
[6] Q. Wu, Y. Liu, Ground temperature monitoring and its recent change in Qinghai–Tibet Plateau, Cold Reg. Sci. Technol. 38 (2) (2004) 85–92.
[7] T.E. Osterkamp, The recent warming of permafrost in Alaska, Global Planet. Change 49 (3) (2005) 187–202.
[8] C. Waelbroeck, Climate-soil processes in the presence of permafrost: a systems modelling approach, Ecol. Model. 69 (3) (1993) 185–225.
[9] O.A. Anisimov, N.I. Shiklomanov, F.E. Nelson, Global warming and active-layer thickness: results from transient general circulation models, Global Planet. Change 15 (3) (1997) 61–77.
[10] V.E. Romanovsky, T.E. Osterkamp, Thawing of the active layer on the coastal plain of the Alaskan arctic, Permafrost Periglac. Process. 8 (1) (1997) 1–22.
[11] N.I. Shiklomanov, F.E. Nelson, Analytic representation of the active layer thickness field, Kuparuk River Basin, Alaska, Ecol. Model. 123 (2) (1999) 105–125.
[12] R. Couture, S.D. Robinson, M.M. Burgess, Climate change, permafrost degradation, and infrastructure adaption: preliminary results from a pilot community case study in the Machenzie valley, Geological Survey of Canada, Current Research 2000-B2 (2000).
[13] Y. Sheng, J. Zhang, Y. Liu, J. Wu, Thermal regime in the embankment of Qinghai–Tibetan highway in permafrost regions, Cold Reg. Sci. Technol. 35 (1) (2002) 35–44.
[14] G.N. Flerchinger, K.E. Saxton, Simultaneous heat and water model of a snow–residue–soil system I. Theory and development, Trans. ASAE 32 (2) (1989) 565–571.
[15] A.T. Degaetano, D.S. Wilks, M. Mckay, A physically based model of soil freezing in humid climates using air temperature and snow cover data, J. Appl. Meteorol. 35 (6) (1996) 1009–1027.
[16] H.S. Carslaw, J.C. Jaeger, Conduction of Heat in Solids, second ed., Oxford University Press, 1986.
[17] G.F. Naterer, Heat Transfer in Single and Multiphase Systems, CRC Press, Boca Raton, FL, 2003.
[18] O.A. Anisimov, N.I. Shiklomanov, F.E. Nelson, Variability of seasonal thaw depth in permafrost regions: a stochastic modeling approach, Ecol. Model. 153 (3) (2002) 217–227.
[19] K.M. Hinkel, J.R.J. Nicholas, Active layer thaw rate at a boreal forest site in central Alaska, USA, Arctic Alpine Res. 27 (1) (1995) 72–80.
[20] J.R. Mackay, Active layer changes (1968 to 1993) following the forest-tundra fire near Inuvik, N.W.T., Canada, Arctic Alpine Res. 27 (4) (1995) 323–336.
[21] F.E. Nelson, N.I. Shiklomanov, G. Mueller, K.M. Hinkel, D.A. Walker, J.G. Bockheim, Estimating active layer thickness over a large region: Kuparuk river basin, Alaska, USA, Arctic Alpine Res. 29 (4) (1997) 367–378.
[22] M.C. Olguín, V.O. Salvadori, R.H. Mascheroni, D.A. Tarzia, An analytical solution for the coupled heat and mass transfer during the freezing of high-water content materials, Int. J. Heat Mass Transfer 51 (17) (2008) 4379–4391.
[23] V.A. Kudryavtsev, L.S. Garagulia, K.A. Kondratyeva, V.G. Melamed, Fundamentals of Frost Forecasting in Geological Engineering Investigations, Nauka, Moscow, Draft Translation 606, Cold Regions Research And Engineering Lab Hanover N H, Hanover, NH, 1977.
[24] J. Brown, K.M. Hinkel, F.E. Nelson, The circumolar active layer monitoring (CALM) program: Research designs and initial results, Polar Geogr. 24 (3) (2000) 165–258.
[25] F.E. Nelson, N.T. Shiklomanov, H.H. Christiansen, K.M. Hinkel, The circumpolar active-layer-monitoring (CALM) workshop: introduction, Permafrost Periglac. Process. 15 (2) (2004) 99–101.
[26] V. Sivanbaev, Thawing of permafrost under a high temperature heat source, Soil Mech. Found. Eng. 8 (1) (1971) 50–53.
[27] L.N. Khrustalev, G.P. Pustovoit, L.V. Emel'yanova, Prediction of permafrost temperature in bed of structure from field data, Soil Mech. Found. Eng. 31 (6) (1994) 200–204.
[28] R. Seshadri, A. Krishnayya, Quasisteady approach for thermal analysis of insulated structures, Int. J. Heat Mass Transfer 23 (1) (1980) 111–121.
[29] M. Krarti, D.E. Claridge, J.F. Kreider, ITPE technique applications to time-varying two-dimensional ground-coupling problems, Int. J. Heat Mass Transfer 31 (9) (1988) 1899–1911.
[30] A. Staudzs, Frost and permafrost: effects and remedial work on transmission tower foundations, Manitoba Hydro (1982).
[31] F. Lefèvre, C.L. Niliot, Multiple transient point heat sources identification in heat diffusion: application to experimental 2D problems, Int. Journal Heat Mass Transfer 45 (9) (2002) 1951–1964.
[32] J.J. Saastamoinen, Unsteady state temperature fields in a slab induced by line sources, Int. Journal Heat Mass Transfer 50 (3) (2007) 756–765.
[33] X. Duan, G.F. Naterer, Ground thermal response to heat conduction in a power transmission tower foundation, Heat Mass Transfer 44 (5) (2008) 547–558.
[34] X. Duan, G.F. Naterer, Ground heat transfer from a varying line source with seasonal temperature fluctuations, ASME J. Heat Transfer 130 (2008). 111302-1-10.
[35] S.J. Kline, F.A. McClintock, Describing uncertainties in single sample experiments, Mech. Eng. 75 (1) (1953) 3–8.
[36] N. Abu-Hamdeh, A. Khdair, R. Reeder, A comparison of two methods used to evaluate thermal conductivity for some soils, Int. J. Heat Mass Transfer 44 (2001) 1073–1078.
[37] J. Lipiec, B. Usowicz, A. Ferrero, Impact of soil compaction and wetness on thermal properties of sloping vineyard soil, Int. J. Heat Mass Transfer 50 (19) (2007) 3837–3847.
[38] Canadian Climate Normals or Averages 1971–2000, Environment Canada, <http://www.climate.weatheroffice.ec.gc.ca/climate_normals/index_e.html>.